SCI INSTITUTE

TECHNICAL REPORT

Physical Mechanisms of DDT in an Array of PBX 9501 Cylinders Initiation Mechanisms of DDT

Jacqueline Beckvermit, Todd Harman, Charles Wight, Martin Berzins

UUSCI-2016-001

Scientific Computing and Imaging Institute
University of Utah
Salt Lake City, UT 84112 USA

April 14, 2016

Abstract:

The Deflagration to Detonation Transition (DDT) in large arrays (100s) of explosive devices is investigated using large-scale computer simulations running the Uintah Computational Framework. Our particular interest is understanding the fundamental physical mechanisms by which convective deflagration of cylindrical PBX 9501 devices can transition to a fully-developed detonation in transportation accidents. The simulations reveal two dominant mechanisms, inertial confinement and Impact to Detonation Transition. In this study we examined the role of physical spacing of the cylinders and how it influenced the initiation of DDT.

Physical Mechanisms of DDT in an Array of PBX 9501 Cylinders

Jacqueline Beckvermit[1]*, Todd Harman[1], Charles Wight[2], and Martin Berzins[1]

[1] University of Utah, Salt Lake City, Utah, U.S.A
[2] Weber State University, Ogden, Utah, U.S.A.

Abstract
The Deflagration to Detonation Transition (DDT) in large arrays (100s) of explosive devices is investigated using large-scale computer simulations running the Uintah Computational Framework. Our particular interest is understanding the fundamental physical mechanisms by which convective deflagration of cylindrical PBX 9501 devices can transition to a fully-developed detonation in transportation accidents. The simulations reveal two dominant mechanisms, inertial confinement and Impact to Detonation Transition. In this study we examined the role of physical spacing of the cylinders and how it influenced the initiation of DDT.

Keywords: DDT, Deflagration, Detonation, Impact to Detonation, Inertial Confinement

1 Introduction

This study of Deflagration to Detonation Transition mechanisms is motivated by an accident that took place in 2005, where a semi tractor trailer carrying 8,400 seismic boosters on US Route 6 in Spanish Fork Canyon Utah, overturned and ignited. Within three minutes, the deflagration caused by the fire transitioned into a fully developed detonation. The detonation produced a crater approximately 24 m wide and 10 m deep; hot metal shards from the trailer started small fires a quarter of a mile away. From the size of the crater it is clear that the explosive underwent a Deflagration to Detonation Transition (DDT). This research is focused on determining the physical mechanisms of a DDT in large arrays of explosive cylinders. This research is significant since the reaction rates of the two modes of combustion (deflagration and denotation) differ by roughly five orders of magnitude, and similar accidents could occur in the future in populated areas.

Many scientists have studied how a subsonic reaction, controlled by heat transfer (deflagration), transitions into a fully developed, highly energetic detonation in a single device. Previous research determined that the different mechanisms for this transition depended, in part, on the porosity and phase of the monolithic solid in a highly confined environment. The mechanisms were studied experimentally [1, 2, 3, 4] and computationally [5, 6]. The physical experiments consist of a condensed phase explosive, packed at various fractions of Theoretical Maximum Densities (TMD), confined in a steel tube. The explosive was ignited by a combustion driven piston moving at low velocities to avoid a shock to detonation transition [1]. Diagnostic probes were placed throughout the steel tube to measure the response of the explosive bed, including but not limited to the velocity of the piston, the velocity of the pressure waves and the onset of convective deflagration. For explosives near the TMD, the mechanism for DDT was the coalescence of pressure waves. In highly confined experiments as described above, the deflagration

*(970)986-2893, 3110 Mount Vernon Ave Apt 224, Alexandria VA 22305, beckvermit@gmail.com

produces pressure waves which propagate through the material, in front of the reaction zone. At some distance the waves coalesce forming a shock discontinuity. This shock continues to grow in strength until the pressure rise causes a transition to detonation [2, 5, 7]. In monolithic solid explosives convective deflagration plays a very important role in the transition, because the pressure waves are generated within the material. Convective deflagration occurs in the cracks and pores of the solid material and is controlled by the convective heat transfer of the penetrating gases [8]. As a result of the pressure waves the explosive undergoes deformation and is damaged allowing the flame to penetrate deeper.

The mechanism for DDT in lower density condensed phase explosives (50-70% TMD) is similar. In the experiments of [1, 4, 7] a porous bed of explosive was ignited by a slow moving piston. The initial compaction wave from the piston traveled through the explosive bed compressing the porous material to around 90% TMD. The frictional hot spots and shear caused by the initial compaction wave ignited the explosive material. Pressure waves formed behind the initial compaction wave further compressing the explosive bed, forming a $\sim$100% TMD high-density plug. This plug was formed in front of the burn front and behind the compaction wave. As the convective deflagration traveled towards the plug, the size of the plug grew. Once the burn front reached the back of the high-density plug it behaved as a second piston, causing a shock to detonation transition in the remaining unburnt explosive [1, 4, 7].

Though the mechanisms for DDT are understood and accepted for highly confined monolithic solids, to our knowledge no research has examined how the shape of the explosive or how the interactions with other explosives influences the transition to detonation. Here we examine arrays of explosive cylinders, specifically those present in the 2005 transportation accident. The explosive of interest is PBX 9501 (95% 1,3,5,7-octahydro-1,3,5,7-tetranitro-1,3,5,7-tetrazocine (HMX) and 5% of a plastic binder) due to the abundance of experimental data and previously validated numerical models for describing DDT [9, 10]. These arrays have gaps between the cylinders providing a pathway for products of reaction to escape and space for cylinders to accelerate and collide with each other unlike a monolithic solid. We therefore expect some similarities to the observed mechanism of porous explosives, with differences due to the interactions with other explosives and the unconfined nature of this problem. The aim of this paper is to present two physical mechanisms for a DDT in multiple large arrays of PBX 9501 cylinders. The two mechanisms are inertial confinement and Impact to Detonation Transition. Section 2 will describe the computational domain and initial conditions, numerical models and present results showing justification for performing 2D simulations. Section 3 will describe the two dominant DDT mechanisms.

2 Computational Methods

To investigate the mechanisms for initiating a DDT in an array of explosives large scale simulations were conducted. These simulations were performed in two and three dimensions. The array consisted of PBX 9501 cylinders, with dimensions similar to those in the 2005 trucking accident, (0.054 m in diameter and 0.33 m long). The size of the cylinders were fixed and the packing configuration was varied see Figure 1. Table 1 describes the different initial configurations for each simulation presented. The compaction and displacement of the explosive cylinders which would be seen in a transportation accident was not examined. This research was focused on determining the initiation mechanism for DDT in an ordered array of explosive cylinders, to understand how deflagration transitions to detonation in the transportation and storage of explosive cylinders. It is understood the movement of the cylinders in the truck rolling over would effect the placement of the cylinders and ultimately the initiation mecha-

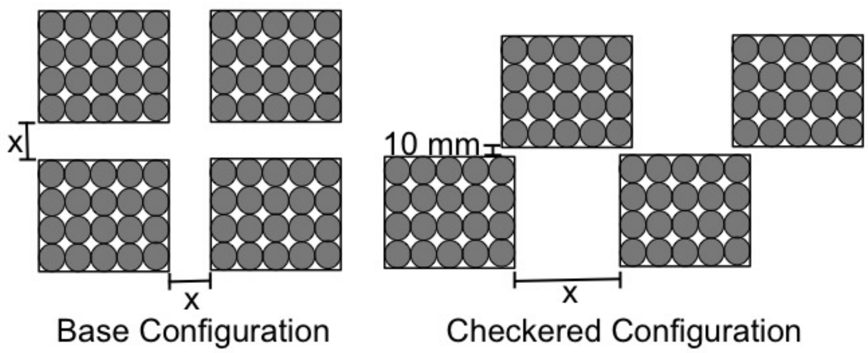

Figure 1: Initial configurations of explosive boxes. Both configurations have 20 cylinders per box.

Table 1: Initial Conditions

Simulation Name	# of Cylinders per box	Spacing between boxes (x)	Configuration (Described in Figure 1)
Transportation Accident	20	10 mm	Base
Base_20_190mm	20	190 mm	Base
Checkered_20_220mm	20	250 mm	Checkered
Base_16_120mm	16	120 mm	Base
Base_12_90mm	12	90 mm	Base
Base_4_14mm	4	14 mm	Base
Base_1_6mm	1	6 mm	Base

nism. The two-dimensional simulations were run with the $x-$, $y-$, $z-$and $z+$ boundaries closed (planes of symmetry), prohibiting gases or explosive particles from escaping. On the $x+$ and $y+$ boundaries we assumed a zero gradient for temperature, pressure, density and velocity. These boundaries were positioned >0.5 m from the reactive explosive to minimize any non-physical boundary condition effects. The initial temperature of the cylinders and surrounding gas was 300 K, and the pressure was 1 atm. To initiate the reactions, the gas temperature in a few computational cells on the $x-$ boundary was set to 2500 K. Adaptive Mesh Refinement and a grid resolution of 2 mm was used to decrease computational costs without loss of fidelity of the results [9, 10, 11]. Resolution studies previously showed that 2 mm grid resolution could be used without degradation to the results [10, 11].

The simulations were all run using the Uintah Computational Framework [12, 13] developed at the University of Utah. This framework utilizes the fluid-structure interaction algorithm of MPM, ICE and MPMICE [14, 15, 16] to solve for the conservation of mass, momentum and energy. The Material Point Method (MPM) is used to evaluate the evolution of the solid material. MPM allows the solid field (Lagrangian points) to distort [15, 17, 18, 19] then they are interpolated back to the cell center in order to be incorporated into the CFD multi-material model (MPMICE). This allows for simulations consisting of multiple phase materials to use the same Eulerian background mesh with no issues related to the laws of conservation. The development and methods for solving the governing multi-material CFD model equations are found in [14, 15, 16, 20, 21]. Embedded within MPMICE is a DDT reaction model. The reaction model has been validated for multiple initial temperatures (273, 298, and 423 K), pressures (0.5-60 MPa) and grid resolutions [9, 10, 11, 22]. The model utilizes a modified Ward, Son and Brewster (WSB) burn model [10, 22, 23] to evaluate the mass conversion rate, the ViscoSCRAM constitutive model [24] to model the damage in the solid, and the JWL++ simple reactive flow model [25] to describe detonation. The DDT model implemented in Uintah does not use the JWL++ model to determine the onset of detonation, it is used to determine the mass conversion rate once detonation is reached. Uintah's DDT model determines when detonation is reached by exceeding a pressure threshold of 5.3 GPa. As described by Peterson et al. [9] this approach gave reasonable run distance to detonation results for shock initiated detonation. The commonly used JWL equation of state [25, 26] was used for the solid explosive and the product gases. A full description of the models used and their limitations can be found in [9].

Substantial changes in the Uintah infrastructure were required in order to run these numerical experiments at the scales required. The MPMICE component, which produces a graph of tasks to be executed, is now done dynamically [27], by using message passing to communicate between nodes [13, 28]. This method has been shown to be portable across a number of different supercomputers, and has been applied to early simulations of the DDT problem considered here [29, 30]. More recently, substantial changes were required to the Uintah infrastructure to allow the large scale simulations described in Section 2.1 [31]. Once these changes were in place, Uintah demonstrated that it is possible to model the 2005 transportation accident [31].

2.1 Dimensional Effects

In this section we provide justification for using low cost 2D computational domains for our investigations, as was done in [31]. Highly resolved 3D simulations are computationally expensive and require tens of thousands of computing cores, running for hundreds of wall clock hours to complete a single simulation. To reduce these costs the effect of the length of the computational domain in the z direction was investigated. Three simulations were performed with z = 3 m (full 3D), 0.33 m (highly confined 3D), and 2 mm (2D). The explosive packing configuration of the 2005 transportation accident, consisting of 20 explosive cylinders packaged in a fiberboard box, was used. For simplicity the fiberboard was not modeled, instead 10 mm gaps filled with air separated the "boxes." In the 2D and highly confined small 3D simulations the $x-, y-, z-$ and $z+$ boundaries were symmetric walls while the $x+$ and $y+$ boundary conditions were a zero gradient for the primitive variables $[T, p, v, \rho]$. Figure 2 shows three domain sizes [31]. The small highly confined 3D domain, yellow region, includes the addition of a 10 mm gaps between the boxes in the z direction. The gap is critical since it allows the hot product gases to expand, similar to the full 3D simulation. Finally, the boundary conditions in the full 3D simulation were planes of symmetry on the $x-$ and $y-$ boundaries, acting as the ground and the back of the truck. All other boundaries conditions were set to a zero gradient for the primitive variables and the edge of the domain was far from the area of interest to minimize, non-physical boundary condition effects.

All three simulations were ignited on the $x-$ axis by hot product gas and they exhibited similar behavior until detonation occurred. We concluded that the DDT resulted from inertial confinement, which will be discussed in Section 3. Figure 3 shows the maximum pressure in the computational domain as a function of time [31]. Note the good qualitative agreement between the three experiments. The oscillations in the pressure profile are due to the deflagration encountering the open space surrounding each cylinder as it traversed through the cylinders.

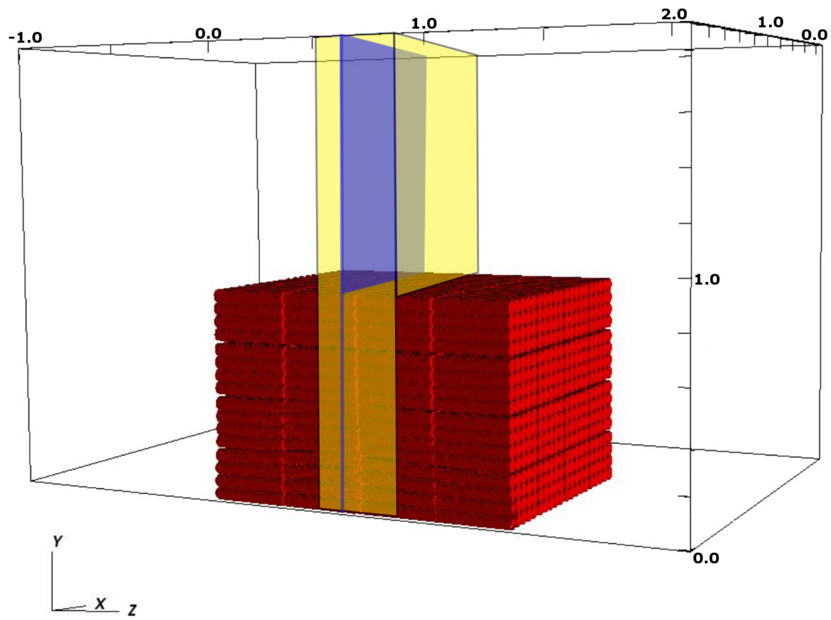

Figure 2: Image illustrating the initial conditions of the 2D (blue), small 3D (yellow) and full 3D (whole image) simulations. The cylinders, red, are packaged in the Transportation Accident configuration, consisting of 20 cylinders per "box".

As expected the large 3D simulation took longer to detonate due to the additional escape routes for expanding product gases. By increasing the length of the$z$dimension the product gases could expand, slowing the rate of pressurization in the domain, and increasing the time to detonation. Not only do the three pressure profiles show similarities the physical location where the DDT took place and the physical mechanism were very similar as shown in Figures 4, 5 and 6. Note that detonation occurred in the same "box" of explosives for all three simulations though in a slightly different position. This is due to the close proximity of the domain walls, preventing product gases from leaving the domain in the 2D and small 3D simulations.

The high computation cost of performing a full 3D simulation and the good quantitative and qualitative agreement in the detonation location and maximum pressure profile justifies using low cost 2D computational domains in this study. The full 3D simulation cost 24M service units ($SU's$) while the small 3D and 2D simulations only cost 215K and 10K $SU's$ respectively.

3 Results and Discussion

The main objective of this paper is to understand the physical mechanisms for a DDT in an array of solid explosives. Two mechanisms were predominantly observed over a wide range of initial conditions, inertial confinement and Impact to Detonation Transition. All simulation results presented used the same sized PBX 9501 cylinders but the initial spacing between the cylinders and "boxes was varied, as described in Table 1 and Figure 1.

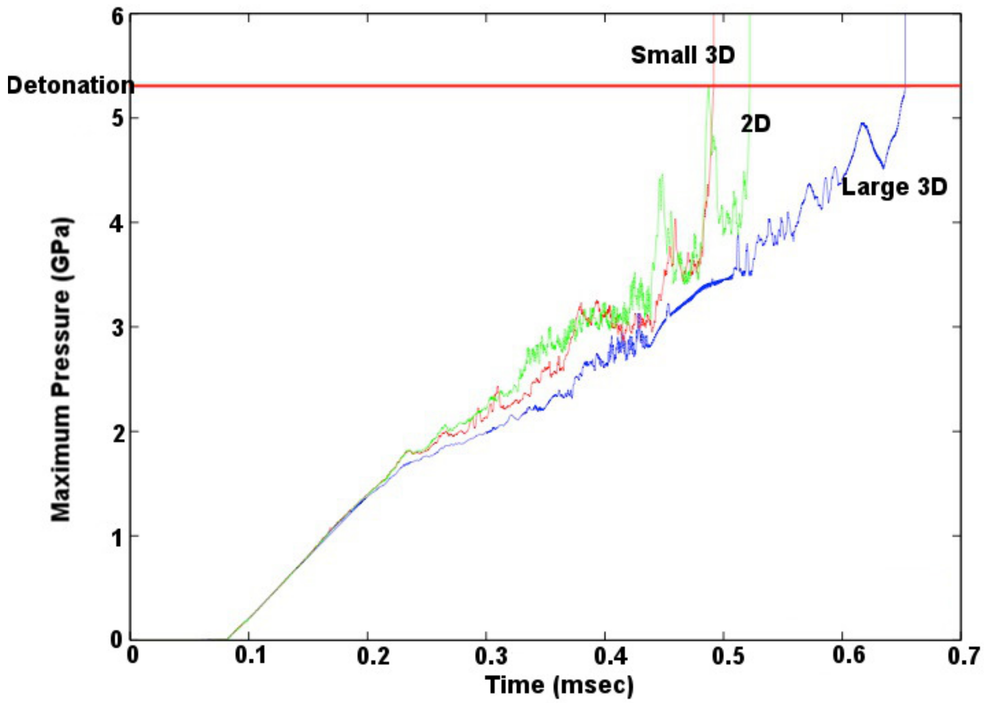

Figure 3: Maximum pressure in the domain versus time for the different sized computation domains.

3.1 Inertial Confinement

Inertial confinement occurs when the inertial mass of the cylinders surrounding a deflagration is greater than the pressure forces exerted on the cylinders. These cylinders move relatively slowly away from the reaction zone and as they move the cylinders collide, and deform filling in the gaps between the cylinders, trapping the product gases. The deformation and expansion of the explosives is limited, due to the close spacing of the cylinders. As deflagration and deformation continues a high-density barrier is formed trapping the product gases, and increasing the local pressure. The increase in localized pressure causes a positive feedback increasing the reaction rate until 5.3 GPa is reached and detonation occurs. This phenomenon is shown in Figure 7, which shows the volume fraction of PBX 9501 after multiple cylinders have deflagrated and deformed. Figure 8 shows the pressure as a function of time and position along the white line in Figure 7. As specified by the reaction model detonation occurs at 5.3 GPa, the red dotted line. Notice that in front of the barrier (0-350 mm) the pressure slowly increases, plateaus then sharply decreases. In these cylinders the product gases flow, unimpeded from the burn front, resulting in a relatively low pressure. The decrease in pressure in these cylinders is sharper than expected due to the cylinders moving through space. Therefore the cylinders from 0-350 mm are slowly decreasing in pressure due to expanding gases and the cylinders moving from the initial position through space while the data is collected at the same point in space. Between 350-480 mm the high density barrier begins to form, restricting the flow field causing an increase in pressure until detonation is reached at 0.753 $msec$. In this region of the domain we observed the explosive cylinders to be moving at approximately 300 m/s as the barrier is being formed, trapping and compressing the gases between the cylinders. A combination of the pressure wave formed from the compression of the gas and the high-density barrier restricting the expansion of product gases is thought to raise the localized internal pressure of the cylinders from 2-3 GPa to detonation. Beyond 480+ mm the cylinders are at ambient pressure and temperature since hot gases cannot flow beyond the barrier.

The inertial confinement mechanism was also observed when 20 cylinders were placed in a "box" and spaced to reproduce the 2005 Transportation Accident, see Figures 4, 5 and 6. Even though the initial layout of the cylinders is different between these simulations the same mechanism to initiate DDT was observed. Visually the barrier is not as pronounced for simulations with 20 cylinders per "box" when compared to simulations consisting of one explosive cylinder per "box." However, in both numerical experiments the explosive material and product gases did not have room to expand, thus the cylinders collided and deformed forming a high-density barrier.

Another way of analyzing the inertial confinement mechanism is looking at the pressure profile in the cell which detonation first occurs, Figure 9. This figure shows the pressure profile for many simulations with varying initial cylinder configurations. For inertial confinement the idealized pressure profile is a monotonic raise in pressure after burning first begins in the cell. The Transportation Accident is a perfect example of this. Notice the pressure in the cell where detonation first occurs gradually increases to 5.3 GPa after ignition, without any sharp transitions. The increase in pressure occurs very quickly after the cell is ignited (less than 1 $msec$). The Base_1_6mm and Base_4_14mm simulations also exhibit this behavior.

With the inertial confinement mechanism the global maximum pressure slowly increases as

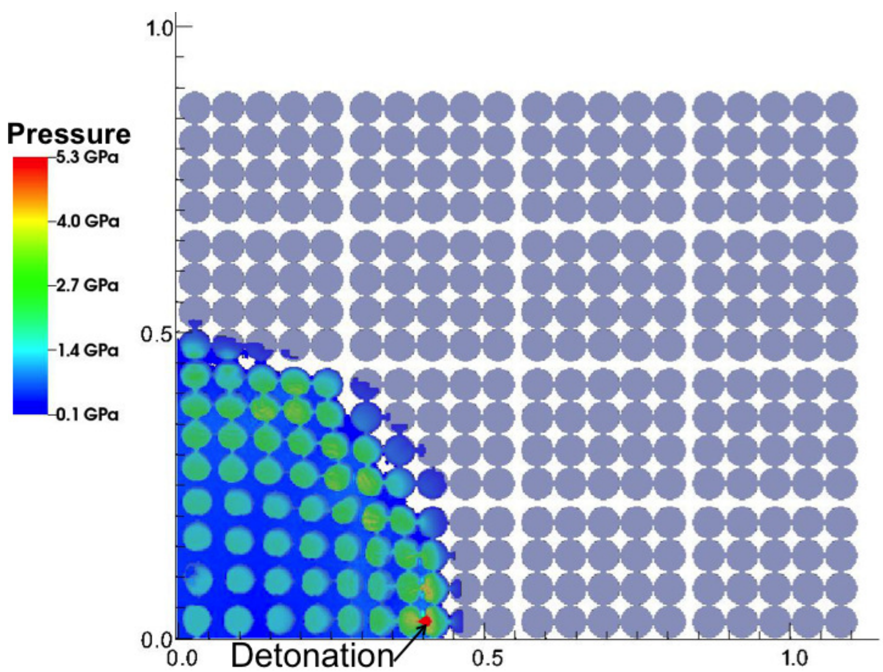

Figure 4: Contour plot of pressure and shadow of explosive cylinders in the 2D simulation (Transportation Accident).

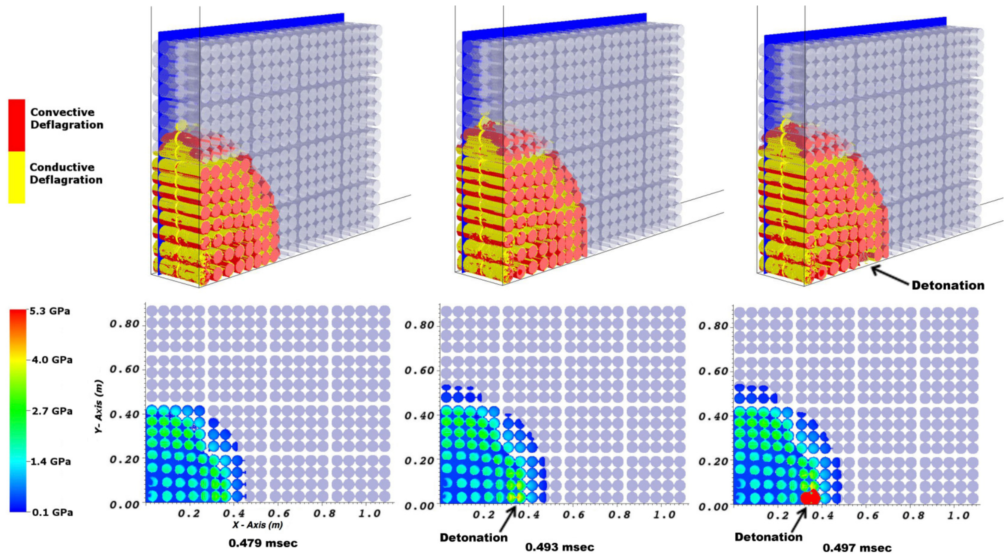

Figure 5: The top figure shows the progression of deflagration through the explosives (light blue). The dark blue slice shows the location of the pressure contour plot (shown below). The bottom plot shows the contour plot of pressure of DDT over time in the small 3D simulation used in [31].

the barrier is formed. This is illustrated in Figure 3 that shows a fairly linear increase in the maximum pressure in the domain until detonation is reached. The amount of time needed

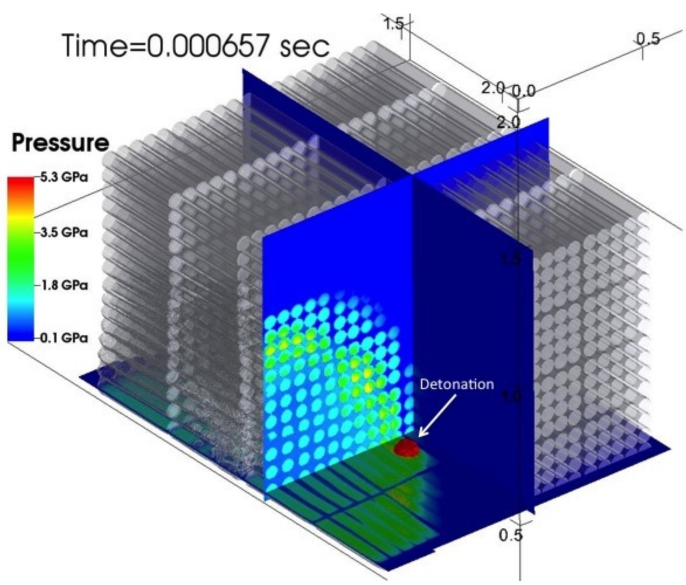

Figure 6: Contour plot of pressure and shadow of the explosive cylinders, in the full 3D simulation.

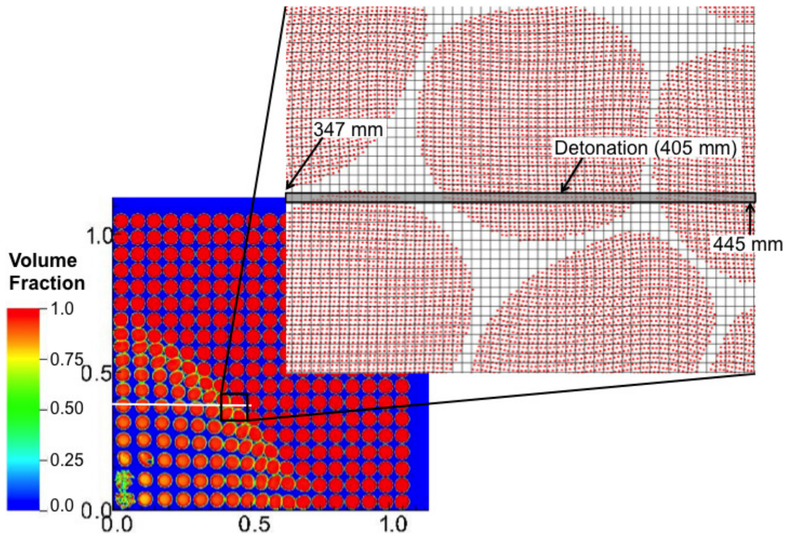

Figure 7: Volume Fraction of PBX 9501 cylinders forming a high-density barrier leading to the inertial confinement mechanism in the Base_1_6mm simulation.

to form this barrier depends on the original configuration of the explosives. As expected the closer the explosives are packaged together the less time it takes to form the barrier. Inertial

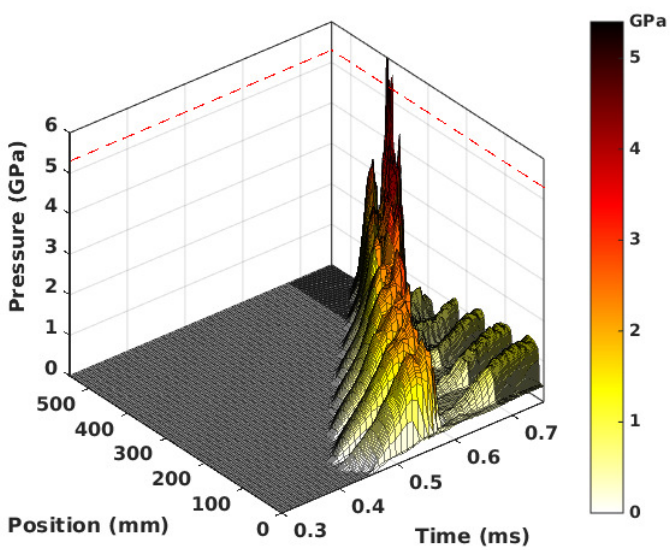

Figure 8: Pressure profile versus position and time. The red dotted line represents detonation. Position of data is shown in Figure 7.

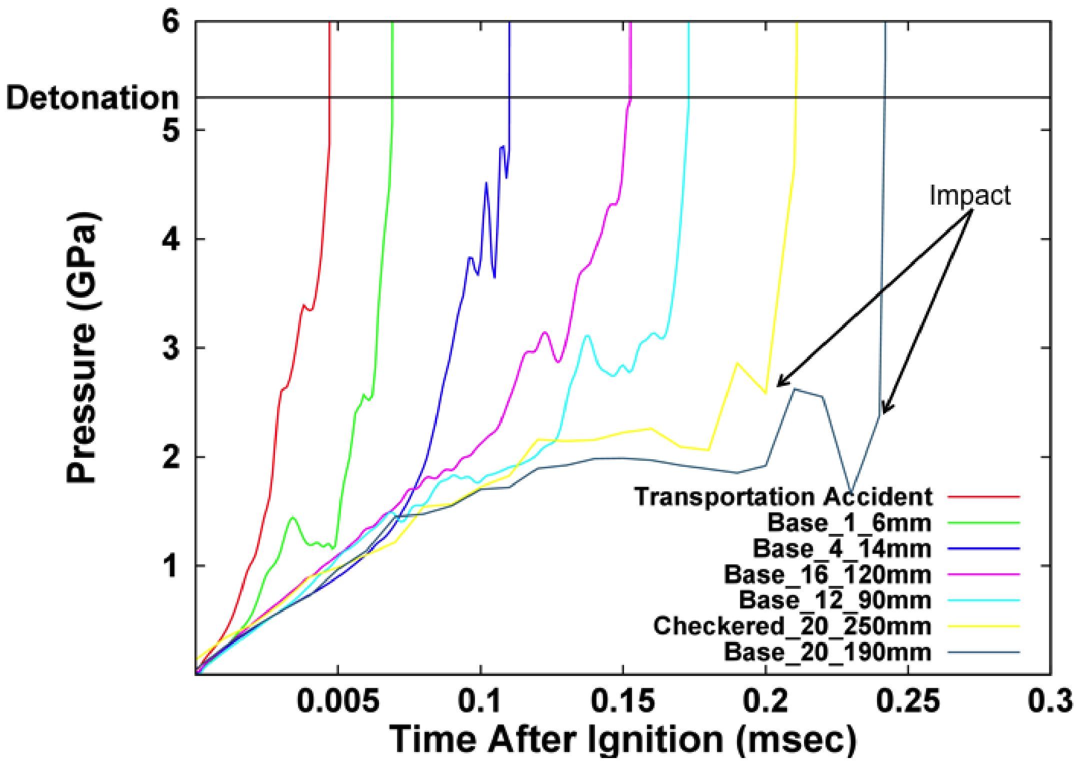

Figure 9: Pressure in cell of detonation after time of ignition.

confinement has only been observed when the explosives are closely packed together. As the explosives are separated there is more room for the explosive material and gases to expand.

3.2 Impact to Detonation Transition

The second mechanism for initiating a DDT in an array of explosive cylinders is an Impact to Detonation Transition (IDT). This occurs when a deflagrating cylinder is impacted by either a) another cylinder or b) by a large pressure wave. When the deflagrating cylinders are at an elevated pressure the external force can be relatively small to initiate a DDT.

The IDT mechanism was observed in simulations where the cylinders were spaced further apart, allowing gases or solids to accelerate before impacting surrounding cylinders. An example of an IDT is shown in Figure 10. The blue region represents surrounding gas and orange region shows high density explosive. As the deflagration moved radially through the domain, deflagrating cylinders began deforming and compacting into one another as seen at point A, forming a "jet" shown at point B. The impact of the solid "jet" caused the transition to detonation. The impact generated stress waves in the explosive that reflected, amplified and accelerated the burn rate to the point of detonation.

Another example of the IDT mechanism was observed when the explosives were packaged 20, (5x4) to a "box." The boxes were evenly spaced 190 mm from one another and separated by

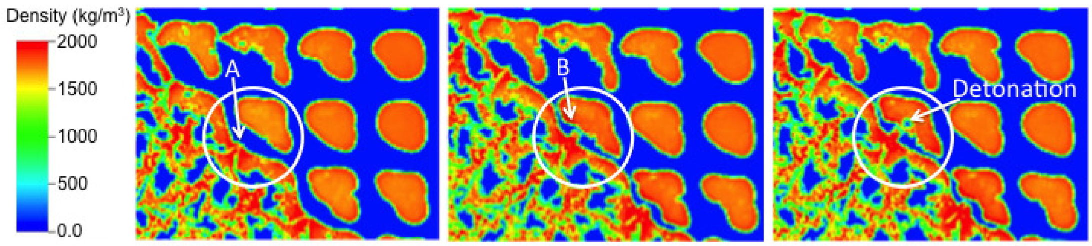

Figure 10: Formation of PBX 9501 "jet" leading to a DDT.

ambient gas (Base_20_190mm simulation). As the deflagration progressed outward from the x-corner of the domain the deflagrating cylinders moved outward accordingly. As shown in Figure 11 the explosive material and gases had ample room to expand. Due to the increased spacing more cylinders had time to deflagrate before the transition to detonation, increasing the overall time to detonation. This simulation detonated 1.55 $msec$ after ignition, more than double the amount of time observed for an inertial confinement DDT. In this simulation the external force or impact was from a pressure wave produced from the deflagration of surrounding explosives. At each cell, shown by the shaded line in Figure 11, a time series of the computed pressure was plotted in Figure 12. Notice the pressure in the deflagrating cylinder, 1630-1644 mm, plateaus around 2 GPa before rapidly increasing to detonation, seen by the red dotted line. This phenomenon is evident in Figure 9, which shows the pressure in the cell where detonation initiated versus time. The pressure profile for this cell, navy blue line, shows the cell deflagrating for a long period of time (2 GPa), before the impact occurred at t=0.24 $msec$ after ignition of the cell. After the impact there is a sharp increase in pressure and detonation occurs.

A third example of the IDT mechanism is shown with 20 cylinders packaged to a "box" arranged in a checkerboard configuration, with 0.25 m gaps between each "box," see Figure 13 (Checkered_20_250mm simulation). As the deflagration progressed outward the product gases and explosive moved away from the origin. At 1.73 $msec$ DDT occurred due to an impact event. Close examination of pressure contour plots and particle visualization showed the impact was a pressure wave and high velocity explosive projectile. Figure 14 shows the pressure profile of this simulation as a function of time and position. In this simulation the pressure in the explosive cylinders was approximately 2 GPa before the impact at which point it rapidly increased to greater than 5.3 GPa. In Figure 9 the yellow line shows the pressure profile in the cell where detonation occurred. It is qualitatively similar to the other experiments with IDT symptoms prior to a DDT.

The Impact to Detonation mechanism was observed in a variety of array layouts. Each experiment exhibited similar traits, a deflagrating cylinder at elevated pressure reaching detonation by an impact. This mechanism was only observed when there was substantial spacing between the boxes or cylinders.

4 Conclusion

Two physical mechanisms for DDT in an array of explosive cylinders were presented, inertial confinement and Impact to Detonation Transition. Inertial confinement occurs when the cylinders are packed closely together allowing for a high-density barrier to form trapping the product gases. Impact to Detonation occurs when deflagrating cylinders at high pressures (1-2 GPa)

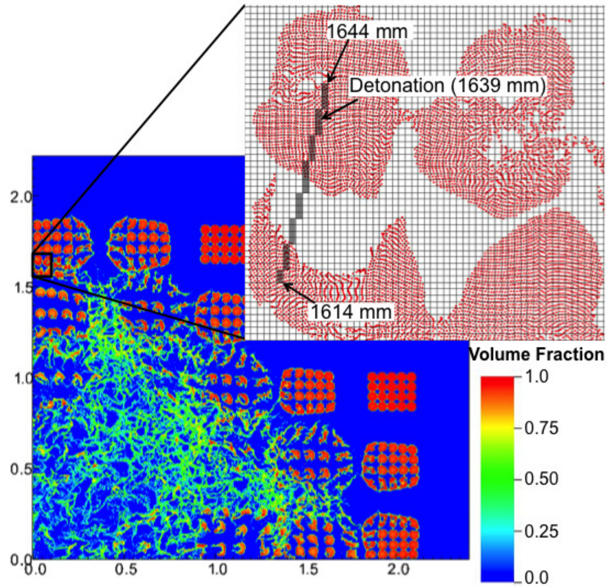

Figure 11: Volume fraction of PBX 9501 in the Base_20_190mm simulation exhibiting IDT mechanism behavior.

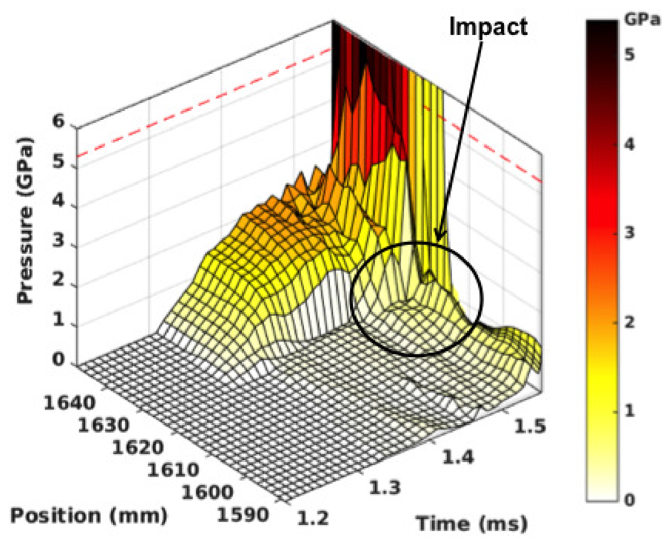

Figure 12: Pressure profile versus time and position for an IDT in Base_20_190mm simulation. Position of data extraction is shown in Figure 11 by the grey region.

undergo a mechanical insult. The differences between these two mechanisms are very subtle and depend on the ability of the product gases to expand. In both mechanisms two conditions are required. First, the cylinders must be at an elevated pressure. For inertial confinement this elevated pressure is much higher than observed in an IDT due to the confinement made

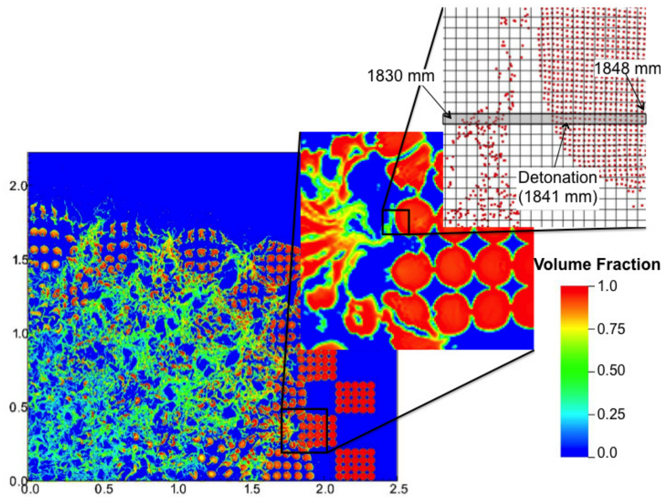

Figure 13: Volume fraction of PBX 9501 in Checkered_20_250mm simulation exhibiting IDT mechanism behavior.

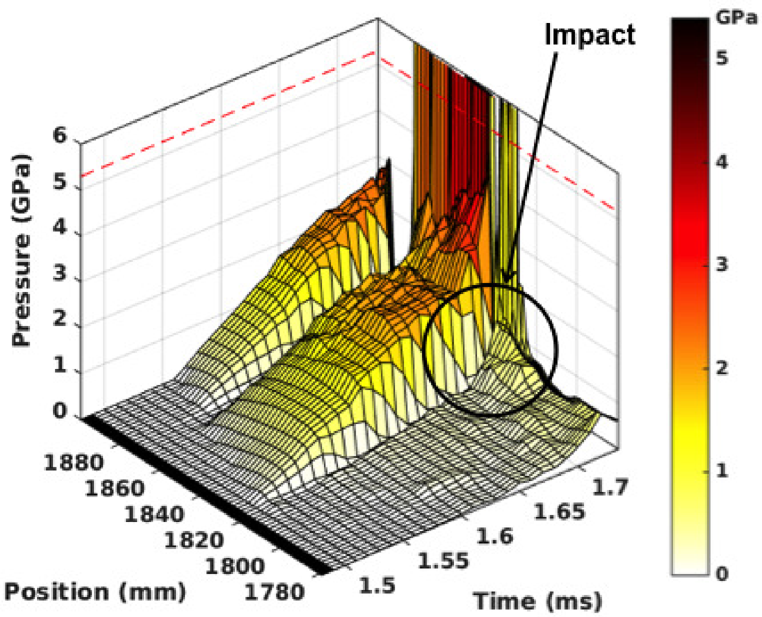

Figure 14: Pressure profile verses time and position for an IDT in the Checkered_20_250mm simulation. Position of data extraction is shown in Figure 13 by the grey region.

from the high-density barrier. Second, there needs to be an external force on the cylinders. With inertial confinement this external force is the compression of trapped gases between the cylinders. For an IDT the force originates from either the impact of pressure waves or fast moving explosive material. The inertial confinement mechanism is easy to identify since the global maximum pressure gradually increases and the cylinders compact together.

Acknowledgments

Uintah was developed by the University of Utahs Center for the Simulation of Accidental Fires and Explosions (C-SAFE) and funded by the Department of Energy, subcontract No. B524196. This work was supported by the National Science Foundation under subcontract No.OCI0721659. An award of computer time was provided by the Innovative and Novel Computational Impact on Theory and Experiment (INCITE) program. This research used resources of the Argonne Leadership Computing Facility at Argonne National Laboratory, which is supported by the Office of Science of the U.S. Department of Energy under contract DEAC02-06CH11357 (sub-award Uintah Safety). This research used resources of the Oak Ridge Leadership Computing Facility at the Oak Ridge National Laboratory, which is supported by the Office of Science of the US DOE under contract DE-AC05-00OR22725 (sub-award ENP009). This work also used the Extreme Discovery Environment (XSEDE), which is supported by NSF grant OCI1053575 (sub-award TGMCA08X004).

References

[1] J. M. McAfee, B. W. Asay, et al., Deflagration to detonation in granular HMX, 9th International Detonation Symposium (1989) 265–279.

[2] A. Macek, Transition from Deflagration to Detonation in Case Explosives, Journal of Chemical Physics 31 (1) (1959) 162–167.

[3] A. Campbell, Deflagration-to-Detonation Transition in Granular HMX, in: JANNAF Propulsion Systems Hazards Subcommittee Meeting, Monterey, CA, 1980, pp. 105–130.

[4] S. F. Son, B. W. Asay, J. B. Bdzil, Inert Plug Formation in the DDT of Granular Energetic Materials, American Institute of Physics (1996) 441–444.

[5] C. M. Tarver, T. C. Goodale, et al., Deflagration-to-Detonation Transition Studies for Two Potential Isomeric Cast Primary Explosives, in: 6th Symposium (International) on Detonation, Coronado, CA, 1976.

[6] R. Gipdon, A. Macek, Flame Fronts and Compression Waves During Transition from Deflagration to Detonation in Solids, in: 8th Symposium (International) on Combustion, Baltimore, MD, 1962.

[7] B. Asay (Ed.), Shock Wave Science and Technology Reference Library, Vol. 5, Springer, 2010.

[8] B. W. Asay, S. F. Son, J. B. Bdzil, The Role of Gas Permeation in Convective Burning, International Journal of Multiphase Flow 22 (5) (1996) 923–952.

[9] J. R. Peterson, C. A. Wight, An Eulerian-Lagrangian Computational Model for Deflagration and Detonation of High Explosives, Combustion and Flame 159 (2012) 2491–2499.

[10] J. Beckvermit, T. Harman, A. Bezdjian, C. Wight, Modeling Deflagration in Energetic Materials using the Uintah Computational Framework, Procedia Computer Science 51 (2015) 552–561.

[11] J. R. Peterson, J. Beckvermit, T. Harman, M. Berzins, C. A. Wight, Multiscale Modeling of High Explosives for Transportation Accidents, in: XSEDE '12: Proceedings of 2012 XSEDE Conference, ACM, New York, NY, 2012.

[12] J. Guilkey, T. Harman, J. Luitjens, J. Schmidt, J. Thornock, J. D. de St. Germain, S. S. J. Peterson, C. Brownlee, C. Reid, T. Saad, J. Beckvermit, A. Humphrey, Uintah Documentaion, http://www.uintah.utah.edu (2015).
URL `http://www.uintah.utah.edu`

[13] Q. Meng, M. Berzins, J. Schmidt, Using Hybrid Parallelism to Improve Memeory use in Uintah, in: TeraGrid 2011 Conference, Salt Lake City, UT, 2011, p. 24.

[14] J. E. Guilkey, T. B. Harman, B. A. Kashiwa, J. Schmidt, P. A. McMurtry, An Eulerian-Lagrangian Approach for Large Deformation Fluid-Structure Interaction Problems, part 1: Algorithm Development, in: Fluid Structure Interactions II, WIT Press, Cadiz, Spain, 2003.

[15] J. E. Guilkey, T. B. Harman, B. Banerjee, An Eulerian-Lagrangian Approach for Simulating Explosions of Energetic Devices, Computers and Structures 85 (2007) 660–674.

[16] T. Harman, J. Guilkey, B. A. Kashiwa, J. Schmidt, P. A. McMurtry, An Eulerian-Lagrangian Approach for Large Deformation Fluid-Structure Interaction Problems, Part 2: Multi-Physics Simulations within a Modern Computational Framework, in: Fluid Structure Interactions II, 2003, pp. 157–166.

[17] D. Sulsky, Z. Chen, H. L. Schreyer, A Particle Method for History Dependent Materials:Dynamic Prioritation of Material Ineterfaces, Computer Methods in Applied Mechanics and Engineering 151 (1998) 343–360.

[18] D. Sulsky, S. Zhou, H. L. Schreyer, Application of Particle-in-Cell Method to Solid Mechanics, Computer Physics Communicaitons 87 (236-252).

[19] S. G. Bardenhagen, E. M. Kober, The Generalized Interpolation Material Point Method, Computer Modeling Engineering and Sciences 5 (477-495).

[20] B. A. Kashiwa, A Multifield Model and Method for Fluid-Stucture Interaction Dynamics, Tech. Report LA-UR-01-1136, Los Alamos National Laboratory (2001).

[21] B. A. Kashiwa, R. M. Rauenzahn, A Multimaterial Formalism, Tech. Report LA-UR-94-771, Los Alamos National Laboratory (1994).

[22] C. A. Wight, E. Eddings, Science-Based Simulation Tools for Hazard Assessment and Mitigation, International Journal of Energetic Materials and Chemical Propulsion 8 (373-389).

[23] M. Ward, S. F. Son, M. Brewster, Steady Deflagration of HMX with Simple Kinetics: A Gas Phase Chain Reaction Model, Combustion and Flame 114 (1998) 556–568.

[24] J. G. Bennett, K. S. Haberman, J. N. Johnson, B. W. Asay, B. F. Henson, A Constitutive Model for the Non-Shock Ignition and Mechanical Response of High Explosives, Journal of the Mechanics and Physics of Solids 46 (12) (1998) 2303–2322.

[25] P. C. Souers, S. Anderson, J. Mercer, E. McGuire, P. Vitello, JWL++: A Simple Reactive Flow Code Package for Detonation, Propellants, Explosives, Pyrotechnics 25 (2000) 54–58.

[26] P. Souers, R. Garza, P. Vitello, Ignition and Growth and JWL++ Detonation Models in Coarse Zones, Propellants, Explosives, Pyrotechnics 27 (62-71).

[27] Q. Meng, J. Luitjens, M. Berzins, Dynamic Task Scheduling for the Uintah Framework, in: in Proceedings of the 3rd IEEE Workshop on Many-Task Computing on Grids and Supercomputers (MTAS10), 2010, pp. 1–10.

[28] Q. Meng, M. Berzins, Scalable Large-Scale Fluid-Structure Interaction Solvers in the Uintah Framework via Hybrid Task-Based Parallelism Algorithms, Concurrency and Computation: Practice and Experience 26 (7) (2014) 1388–1407.

[29] M. Berzins, J. Luitjens, Q. Meng, T. Harman, C. A. Wight, J. R. Peterson, Uintah: A Scalable Framework for Hazard Analysis, in: Proceedings of the Teragrid 2010 Conference, TG 10, 2010.

[30] J. Beckvermit, J. Peterson, T. Harman, S. Bardenhagen, C. Wight, Q. Meng, M. Berzins, Multiscale Modeling of Accidental Explosions and Detonations, Computing in Science and Engineering 15 (4) (2013) 76–86.

[31] M. Berzins, J. Beckvermit, T. Harman, A. Bezdjian, A. Humphrey, Q. Meng, J. Schmidt, C. Wight, Extending the Uintah Framework to Enable Petascale Modeling of Detonation in Arrays of High Explosive Devices, Accepted to SIAM Journal on Scientific Computation.